ANNALS of Faculty Engineering Hunedoara
– International Journal of Engineering

Tome XII [2014] – Fascicule 3 [August]
ISSN: 1584-2673 [CD-Rom, online]

a free-access multidisciplinary publication
of the Faculty of Engineering Hunedoara

[1.] Ton That Hoang LAN

A NURBS BASED FEM FOR THE CONVECTION – DIFFUSION PROBLEMS UNDER ISOGEOMETRIC ANALYSIS

[1.] Department of Civil Engineering, University of Architecture, HoChiMinh City, VIETNAM

Abstract: There are several technologies available to the Isogeometric Analysis (IGA) framework, of which NURBS is most commonly used since it is the standard technology employed in CAD programs. NURBS generalize B-Splines and consequently inherit all of their favourable properties for free-form design. NURBS are commonly used in Computer Aided Design (CAD), Manufacturing (CAM), and Engineering (CAE) and are part of numerous industry-wide used standards, such as IGES, STEP, ACIS, and PHIGS. NURBS are piecewise-rational functions and allow a compact representation of geometry, can exactly represent some simple geometries like cylinders, spheres, ellipsoids and allow easy manipulation through their control points. Isogeometric Analysis (IGA) based on NURBS has refinement procedures analogue to *h*- and *p*-refinement in FEA, which are respectively known as knot insertion and degree elevation. The property of splines having a high level of derivative continuity at element interfaces also gives rise to the potentially more powerful *k*-refinement, where the degree is elevated together with the continuity at the element interfaces. In this study will show the development of a NURBS based FEM for the convection-diffusion problem under Isogeometric Analysis (IGA). Numerical results are performed on the convection-diffusion equation.
Keywords: Nurbs, Fem, Convection-Diffusion, IGA

1. INTRODUCTION

Isogeometric Analysis (IGA) was introduced in 2005 by Hughes et al. [8] to bring exact engineering geometry to Finite Element Analysis (FEA) and alleviate the cumbersome process of meshing altogether. The Isogeometric Analysis (IGA) concept unifies the two fields of CAD and FEA by expanding the solution space using the same basis as that of the geometry description from CAD. Since its introduction, IGA has successfully been applied to a wide variety of problems in structural analysis [9, 10, 11], electromagnetics [12], turbulence [1, 13, 14], fluid structure interaction [3, 4, 6, 7] and higher order partial differential equations [5]. NURBS offer almost spectral approximation properties and all modes converge with increasing order of approximation. These are very desirable properties in problems with wave propagation, long time integration and a multi-scale character. These properties are mainly ascribed to the aforementioned inter-element continuity of the basis functions.

2. NON-UNIFORM RATIONAL B-SPLINES (NURBS)

B-splines have their rational counterparts giving the ability to exactly represent objects that cannot be represented by polynomials. For example in CAD circular and conic shapes are often used, which can be exactly represented by NURBS. The NURBS basis is defined by associating the B-spline basis functions with a strictly positive weight, ω_i as

$$N_{i,p}(\xi) = \frac{\omega_i B_{i,p}(\xi)}{W(\xi)} \tag{1}$$

where

$$W(\xi) = \sum_{1}^{n} \omega_i B_{i,p}(\xi) \tag{2}$$

spanning the NURBS function space uniquely defined as $N \equiv N(\Xi; p; \omega) := span\left\{ N_{i,p} \right\}_{i=1}^{n}$ Analogous to B-Splines higher dimensional function spaces are constructed using tensor products of univariate basis functions $N \equiv N(\Xi; H; ...; p; q; ...; \omega) := span\left\{ N_{i,p} \otimes N_{j,q} \otimes ... \right\}_{i,j,...=1}^{n,m,...}$

The NURBS basis has the following properties: *i).* The NURBS basis constitutes a partition of unity $\sum_{1}^{n} N_{i,p}(\xi) = 1$; *ii).* NURBS inherit their properties from the B-Spline basis functions like continuity across knots, local support and non-negativity. *iii).* The NURBS basis functions are not polynomial but rational functions. *iiii).* If the weights are all equal the basis is again polynomial. Hence, B-Splines are a special case of NURBS. NURBS derivatives are found by using the quotient rule on (1), expressing the derivative in the B-Spline basis, namely

$$\frac{d}{d\xi} N_{i,p}(\xi) = \omega_i \frac{W(\xi) B'_{i,p}(\xi) - W'(\xi) B_{i,p}(\xi)}{(W(\xi))^2} \tag{3}$$

where $B'_{i,p}(\xi) \equiv \frac{d}{d\xi} B_{i,p}(\xi)$ and $W'(\xi) = \sum_{1}^{n} B'_{i,p}(\xi) \omega_i$. Now define $A^{(k)}{}_i(\xi) = \omega_i \frac{d^k}{d\xi^k} B_{i,p}(\xi)$, no sum on i and let $W^k(\xi) = \frac{d^k}{d\xi^k} W(\xi)$

Then higher order derivatives are expressed in terms of lower orderderivatives as

$$\frac{d^k}{d\xi^k} N_{i,p}(\xi) = \frac{A_i^{(k)}(\xi) - \sum_{j=1}^{k} \binom{k}{j} W^{(j)}(\xi) \frac{d^{(k-j)}}{d\xi^{(k-j)}} N_{i,p}(\xi)}{W(\xi)} \text{ where } \binom{k}{j} = \frac{k!}{j!(k-j)!} \tag{4}$$

Using (1) the NURBS curve can be defined in the same way as the B-Spline curve namely

$$C(\xi) = \sum_{i=1}^{n} N_{i,p}(\xi) P_i \tag{5}$$

Figure 1 shows the construction of a circular arc. Note that one weight has the value $1/\sqrt{2}$ to allow exact representation of the circle. The dashed line showsthe curve when all weights are equal to one and hence this curve is polynomial. Comparing the two curves it is clear that due to the weight the middle control point pulls the curve less strong.

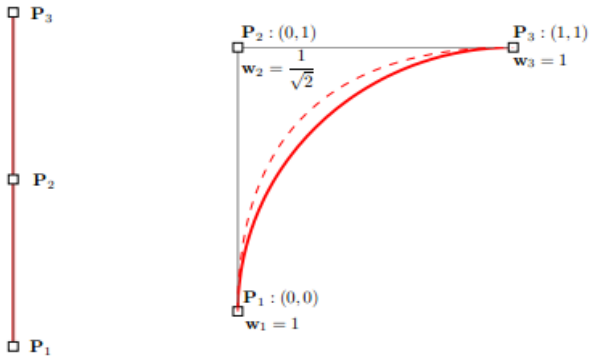

Figure 1: Example of the construction of a NURBS quarter circle curve based on the knot vector Ξ ={0,0,0,1,1,1}. The dashed line indicates the unweighed curve

In an analogous way the NURBS surface and NURBS solid are defined as

$$S(\xi, \eta) = \sum_{i=1, j=1}^{n,m} N_{i,p}(\xi) N_{j,q}(\eta) P_{i,j} \tag{6}$$

and

$$V(\xi, \eta, \varsigma) = \sum_{i=1, j=1, k=1}^{n,m,l} N_{i,p}(\xi) N_{j,q}(\eta) N_{k,r}(\varsigma) P_{i,j,k} \tag{7}$$

Figure 2 shows the construction of a circular surface by a mapping from parameter space to physical space using the control points and weights of the circular arc, Figure 1, for each side of the parameter space forming a circular surface in physical space.

3. A NURBS BASED FEM FOR THE CONVECTION – DIFFUSION EQUATION UNDER ISOGEOMETRIC ANALYSIS (IGA)

Before going to the main, Table1 summarizes the important differences and similarities between FEM and IGA.

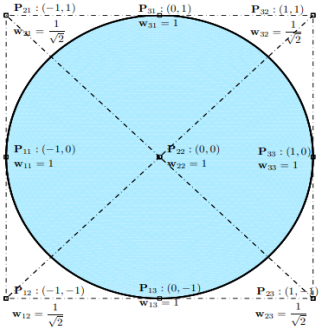

Figure 2: Construction of a circle using NURBS. The surface is constructed using the knot vectors Ξ =H={0,0,0,1,1,1}and control points and weights as shown in the figure.

Table 1: Comparison of FEM and IGA summarizing the differences and similarities between FEM and IGA

FEM		IGA
Nodal points		Control points
Nodal variables		Control variables
Mesh		Knots
Element		Knot span
Basis interpolates nodal points and variables		Basis doesnotinterpolate control points and variables
Approximate geometry	Compact support	Exact geometry
Polynomial basis	Partition of unity	NURBS basis
Gibbs phenomena	Isoparametric concept	Variation
Subdomains	Affine covariance	Diminishing
	Patch tests satisfied	Patches

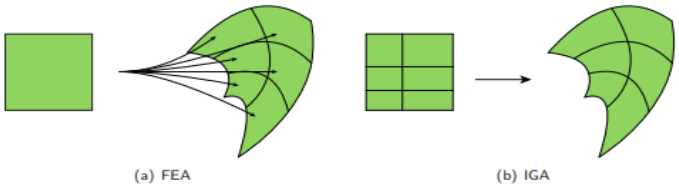

Figure 3: In classical FEA, Figure 3(a), the parameter space is local to elements. Each element has its own mapping from parameter space to physical space. In IGA, Figure 3(b), the parameter space is local to patches. Internal knots partition the parameter space in elements. A single B-Spline or NURBS maps parameter space to physical space.

Figure 3 illustrates what this implies from an analysis point of view. In classical FEM each element has its own mapping from parameter space to physical space, Figure 3(a). While in IGA, internal knots partition the parameter space in elements and a single B-Spline maps parameter space to physical space, Figure 3(b).

The mesh in IGA is directly defined by the NURBS parametrization. Let Ω' be an open bounded domain with a boundary $\partial\Omega'$. The domain is divided into subdomains $\Omega' \cup_e \Omega'_e$ by quadrilaterals such that $\Omega'_i \cap \Omega'_j = 0$ for $i \neq j$. The elements are defined as the knot spans, $\Omega'_e = \{[\xi_i, \xi_{i+1})\}$ or tensor products thereof, $\Omega'_e = \{[\xi_i, \xi_{i+1}) \otimes [\eta_i, \eta_{i+1}) \otimes \ldots\}$ in higher dimensions. The element in physical space is defined as $\Omega_e = S \circ \Omega'_e$, where S is the NURBS map in [8].

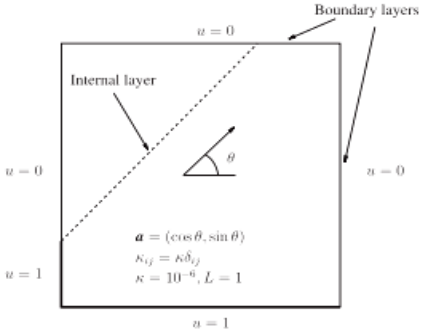

Figure 4: Problem description

Consider the convection-diffusion equation on a domain Ω, Figure 4:

$$-\kappa\Delta u(x,y) + a\nabla u(x,y) = f(x,y) \text{ in } \Omega \qquad (8)$$

$$u = g(x,y) \text{ on } \Gamma$$

where u(x,y) is the concentration of a pollutant, κ is the diffusivity tensor, a is the convection velocity and f(x,y) is a source term. The Galerkin method is used for the discretization of the convection-diffusion problem. The needed function spaces are defined here, for the weak formulation and variational form. Define a collection of trial solutions S, required to be square integrable and to satisfy the boundary conditions:

$$S = \left\{ u \middle| u \in H^1(\Omega), u\middle|_\Gamma = g(x,y) \right\} \qquad (9)$$

Next define a collection of weighting functions v

$$v = \left\{ \omega \middle| \omega \in H^1(\Omega), \omega\middle|_\Gamma = 0 \right\} \qquad (10)$$

where $\omega = \omega(x,y)$. The Sobolev space, H^1, induces the following $L_2(\Omega)$ inner product and norm, viz

$$(u,v) = \int_\Omega uv d\Omega \text{ and } \|u\|_2 = (u,v)^{1/2} \qquad (11)$$

Let the solution space consist of all linear combinations of a given set of NURBS functions $N_A: \Omega \rightarrow R$, where A= 1,... ,$n_{np}$. Where N_A denotes the tensor product of univariate NURBS basis functions, with A being the global equation number connected to the local numbering through the "NURBS coordinates array" (INC-array)[2]. Using the compact support property of the functions and assuming that there exists an integer $n_{eq} < n_{np}$ such that

$$N_{A|\Gamma} = 0 \quad \forall A = 1,\ldots,n_{eq} \tag{12}$$

Hence, for all $\omega^h \in v^h$, there exist constants c_A, A= 1,... ,n_{eq} such that

$$\omega^h = \sum_{A=1}^{n_{eq}} N_A(x,y) c_A \tag{13}$$

Then require that each $N_A(x,y)$ satisfies

$$N_A(1) = 0 \quad \forall A = 1,\ldots,n_{eq} \tag{14}$$

from which it follows by (13) that $\omega^h(1) = 0$. Hence v^h has dimension n_{eq}.

Next to define members of S^h we need to specify g^h (a "lifting"), therefore we introduce the coefficients g_A, A = 1,... ,n_{np}. Note that it is convenient to choose g^h such that $g_1 = \ldots = g_{neq} = 0$ as they have no effect on its value on Γ. So,

$$g^h = \sum_{A=n_{eq}+1}^{n_{np}} N_A(x,y) g_A \tag{15}$$

Now apply variational form, such that for any $u^h \in S^h$ there exist a d_A, A = 1,... ,n_{eq} such that

$$u^h = \sum_{A=1}^{n_{eq}} N_A(x,y) d_A + \sum_{B=n_{eq}+1}^{n_{np}} N_B(x,y) g_B = \sum_{A=1}^{n_{eq}} N_A(x,y) d_A + g^h \tag{16}$$

Finally combine (13), (16) and exploit linearity to obtain the expression

$$\sum_{A=1}^{n_{eq}} c_A \left\{ \sum_{B=1}^{n_{eq}} d_B \left(\int \nabla N_A(x,y) \kappa \nabla N_B(x,y) + a N_A(x,y) \nabla N_B(x,y) d\Omega \right) - \right. \\ \left. - \int_\Omega N_A(x,y) f d\Omega + \sum_{B=n_{eq}+1}^{n_{np}} g_B \left(\int_\Omega \nabla N_A(x,y) \kappa \nabla N_B(x,y) + a \nabla N_A(x,y) \nabla N_B(x,y) d\Omega \right) \right\} = 0 \tag{17}$$

The Galerkin equation has to hold for all $\omega^h \in v^h$. By (13), this means for all c_A, A = 1,... ,n_{eq}. Since the c_A's are arbitrary in (17) it follows that the term between braces must vanish. Hence, for A= 1,... ,n_{eq} , dropping arguments for brevity,

$$\sum_{B=1}^{n_{eq}} d_B \left(\int_\Omega \nabla N_A \kappa \nabla N_B + a N_A \nabla N_B d\Omega \right) = \int_\Omega N_A f d\Omega - \sum_{B=n_{eq}+1}^{n_{np}} g_B \left(\int_\Omega \nabla N_A \kappa \nabla N_B + a N_A \nabla N_B d\Omega \right) \tag{18}$$

Now further define the matrix system,

$$K_{AB} = \int_\Omega \nabla N_A \kappa \nabla N_B + a N_A \nabla N_B d\Omega$$
$$F_A = \int_\Omega N_A f d\Omega - \sum_{B=n_{eq}+1}^{n_{np}} g_B \left(\int_\Omega \nabla N_A \kappa \nabla N_B + a N_A \nabla N_B d\Omega \right) \tag{19}$$

Then (18) becomes, after inclusion of the Dirichlet conditions,

$$\sum_{B=1}^{n_{eq}} K_{AB} d_B = F_A \qquad A = 1,\ldots,n_{eq} \tag{20}$$

Or, using matrix notation

$$K = [K_{AB}]; \quad d = \{d_B\}; \quad F = \{F_A\}$$

to obtain the form

$$Kd = F \tag{21}$$

where the Dirichlet condition will be treated slightly different in practice by choosing a numbering such that

$$\begin{bmatrix} K_{11} & K_{12} \\ K_{21} & K_{22} \end{bmatrix} \begin{Bmatrix} d_B \\ g_B \end{Bmatrix} = \begin{Bmatrix} F_A \\ F_{gB} \end{Bmatrix} \tag{22}$$

Then the system can be solved as follows, viz

$$K_{11}d_B = F_A - K_{12}g_B \tag{23}$$

The assembly process takes the following form in terms of the local "node" numbers 1≤ a,b ≤n_{en},

$$K = \mathrm{A}^e K_{ab}^e \quad K_{ab}^e = \int_{\Omega_e} \nabla N_a \kappa \nabla N_b + a N_a \nabla N_b d\Omega \quad F = \mathrm{A}^e F_{ab}^e \quad f_a^e = \int_{\Omega_e} N_a f d\Omega \tag{24}$$

where A is the assembly operator. Defining $B_a = \nabla N_a = \begin{bmatrix} N_{a,x}(x,y) \\ N_{a,y}(x,y) \end{bmatrix}$ then the component version becomes

$$K_{ab} = \int_{\Omega} B_a^T \kappa B_b + a^T N_a(x,y) B_b d\Omega \tag{25}$$

The quadrature points and their weights are provided by Gauss-Legendre quadrature. The solution is $d = K^{-1}(F_A - K_{12}g_B)$, assuming that K is invertible. Once d is known, the solution can be constructed at any point $x, y \in \Omega$ using the NURBS basis, namely

$$u^h = \sum_{A=1}^{n_{np}} N_A(x,y) d_A \tag{26}$$

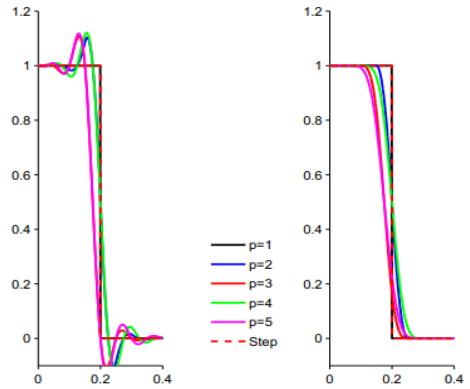

Figure 5: Imposition of strong boundary conditions on the west boundary of the convection diffusion problem. The left hand figure shows interpolation of the discontinuous data. Note that NURBS also exhibit the Gibbs phenomenon, though much less than Lagrange polynomials due to the variation diminishing property of the B-Spline basis. The right hand figure shows imposition of the data directly on the control points. Note how the boundary condition gets smeared for increasing p.

Boundary conditions in IGA are imposed in the same way as in a classical FEM. The essential boundary conditions are imposed on the control points. Because NURBS are non interpolatory strong boundary conditions tend to get smeared for higher order basis functions when discontinuous boundary data is imposed. Figure 5 shows this for a step profile which corresponds to the west boundary conditions in the convection-diffusion problem. On the left an interpolation of these conditions is shown, on the right the conditions are directly imposed on the control points. Note that although NURBS have the variation diminishing property they still exhibit the Gibbs phenomenon, but gets less for increasing degree as opposed to polynomials. Furthermore note how the data gets smeared for increasing p. It is obvious that for discontinuous data it is better to impose the data directly on the control points. The converse is true when smooth data is considered. If this smearing is unacceptable a better lifting can be found by a curve or surface fitting algorithm using a least squares approach. Another option is to impose Dirichlet conditions weakly. Although this is an approximation of the Dirichlet condition, it comes with great advantages. In problems with boundary layer phenomena for instance, it can help to eliminate spurious oscillations [2]. In addition the strong imposition is also an approximation due to the smearing effect, thus one can argue which method is better.

For the assembly of the stiffness and mass matrix and the load vector the following general integral must be performed

$$\int_{\Omega_e} f(x) d\Omega \tag{27}$$

where f is assumed sufficiently smooth and integrable. To facilitate the integration, the integrals are pulled from physical space to the parent element. In order to do this a change of variables has to be performed, in 1D this becomes

$$\int_{\tilde{\Omega}} f(\tilde{\xi}) \frac{dx}{d\xi} \frac{d\xi}{d\tilde{\xi}} d\tilde{\Omega} \tag{28}$$

and in 2D

$$\int_{\tilde{\Omega}} f(\tilde{\xi}, \tilde{\eta}) J_S \| J_\psi | d\tilde{\Omega} \tag{29}$$

where J is the Jacobian and |J| is the Jacobian determinant.

For a typical stiffness matrix component $f(x,y)=\nabla N_A(x,y)\kappa\nabla N_B(x,y)$. The basis functions N are defined in the parameter space Ω' in order to define the basis in Ω we need the derivative of the pull back $DS^{-1}=J_S^{-1}$ and apply the chain rule, viz

$$\nabla N(x,y)=J_S^{-1}\nabla N(\xi,\eta) \tag{30}$$

Now the integral becomes

$$\int_{\tilde{\Omega}}\left(J_S^{-1}\nabla N_A\left(\tilde{\xi},\tilde{\eta}\right)\right)\kappa\left(J_S^{-1}\nabla N_B\left(\tilde{\xi},\tilde{\eta}\right)\right)\left|J_S\right|\left|J_\psi\right|d\tilde{\Omega} \tag{31}$$

Lets perform the integration of (28) numerically, viz

$$\int_{\tilde{\Omega}} f\left(\tilde{\xi}\right)\frac{dx}{d\xi}\frac{d\xi}{d\tilde{\xi}}d\tilde{\Omega}=\sum_{i=1}^{n_{ip}}W_i f\left(\hat{\xi}_i\right)\frac{dx}{d\xi}\frac{d\xi}{d\tilde{\xi}}+r\approx\sum_{i=1}^{n_{ip}}W_i f\left(\hat{\xi}_i\right)\frac{dx}{d\xi}\frac{d\xi}{d\tilde{\xi}} \tag{32}$$

where n_{ip} are the number of integration points $\hat{\xi}_i$, W_i is the weight corresponding to the i^{th} integration point and r is a residual. Gaussian quadrature is optimal in a sense that it integrates a function accurately with the least amount of quadrature points. The B-spline basis fulfils the smoothness and integrability conditions and is polynomial so standard Gauss rules can be applied.

The last will showcase numerical results for the linear convection-diffusion equation. The linear convection-equation is discretized. The quality of the solution is measured in the $L_2(\Omega)$-norm defined as

$$L_2(\Omega)=\sqrt{\int_\Omega\left(u^a-u^h\right)^2 d\Omega} \tag{33}$$

where u_a is the analytical solution. The h-convergence results are plotted against the maximum element circumdiameter denoted as h_{max}. For the linear convection-diffusion case only qualitative results will be shown. The meshes used for the numerical results are shown in Figure 6, Figure 7, Figure 8 and Figure 9.

The convection-diffusion problem (8) is solved for $\kappa=10^{-6}$, $a=(\cos\theta,\sin\theta)$ with $\theta=45^\circ$. The stability parameter was chosen as $\tau=h_a/2a$, where $h_a=\frac{h}{\max\{\cos\theta,\sin\theta\}}$, the element length in the flow direction.

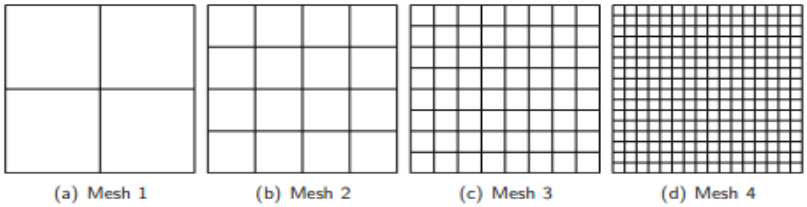

Figure 6: Refinement sequence for the unit square.

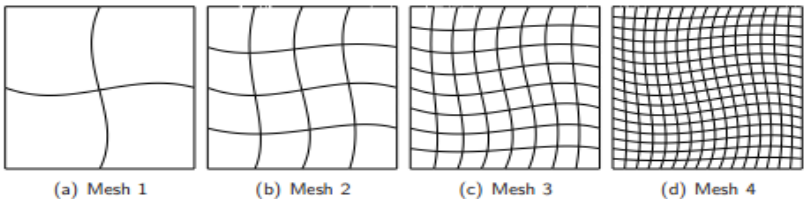

Figure 7: Refinement sequence for curvilinear 1

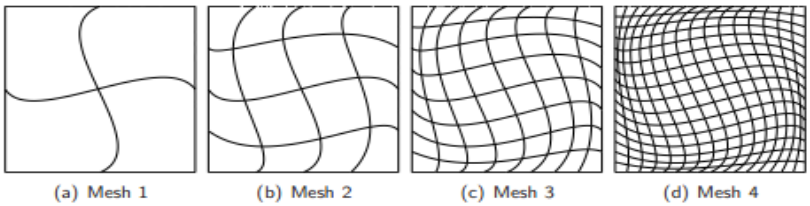

Figure 8: Refinement sequence for curvilinear 2

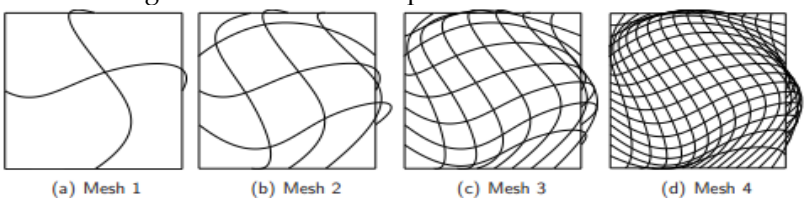

Figure 9: Refinement sequence for curvilinear 3

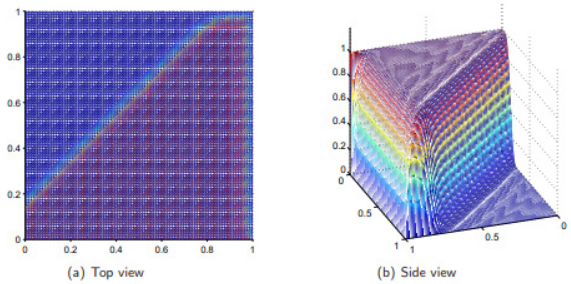

Figure 10: Convection-diffusion at 45 degrees flow angle for mesh 4 of Figure 6 at p= 4. Clearly visible is the smearing of the sharp layer and boundary conditions. Note further the smoothness of the solution due to the variation diminishing property

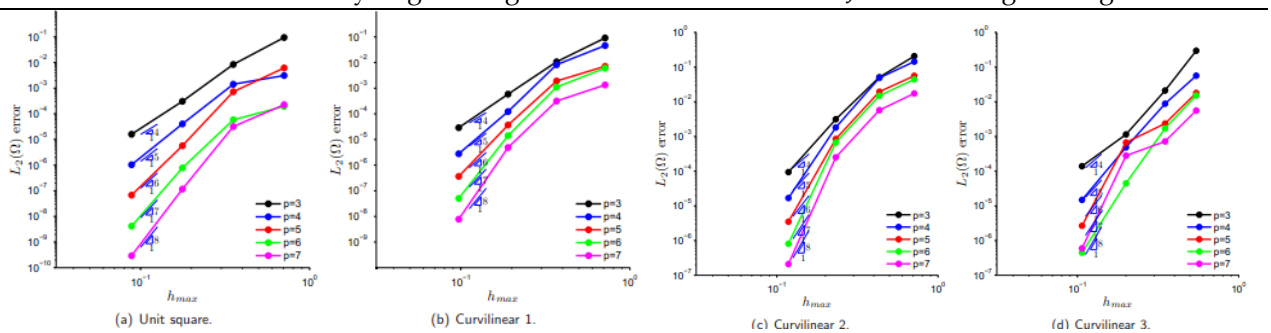

Figure 11: Convergence in the $L_2(\Omega)$ norm versus h_{max}.

It is clear that on all meshes optimal convergence rates are attained.

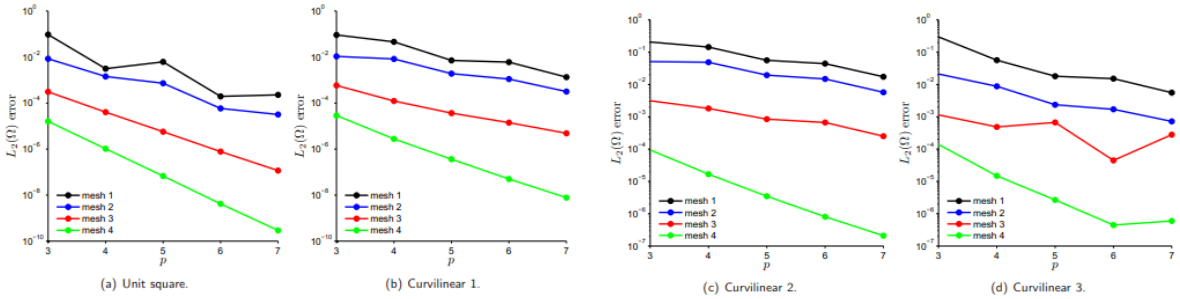

Figure 12: Convergence in the $L_2(\Omega)$ norm versus p.

4. CONCLUSION

In Isogeometric Analysis (IGA) elements are defined in the parameter domain by the knot spans. The development of a FEM based on NURBS is equal to a classical FEM. Differences are introduced when imposing boundary conditions. Boundary conditions can be imposed directly on the control points or by interpolation. For discontinuous data it is beneficial to impose the boundary conditions to the control points directly. In the convection diffusion problem the sharp layers are smeared due to the properties of the basis. Furthermore the solution is smooth due to the variation diminishing property. The conditioning of the stiffness matrix is constant with degree. Furthermore, poor conditioning has no implications on the accuracy of the solution.

References

[1.] I. Akkerman, Y. Bazilevs, VM Calo, T.J.R. Hughes, and S.J. Hulshoff. The role of continuity in residual-based variational multiscale modeling of turbulence. Computational Mechanics, 41(3):371–378, 2008. ISSN 0178-767.

[2.] Y. Bazilevs and T.J.R. Hughes. Weak imposition of Dirichlet bound-ary conditions in fluid mechanics. Computers Fluids, 36(1):12 – 26, 2007. ISSN 0045-7930. doi: 10.1016/j.compfluid.2005.07.012. URL http://www.sciencedirect.com/science/article/pii/S0045793005001258. Challenges and Advances in Flow Simulation and Modeling.

[3.] Y. Bazilevs, V.M. Calo, Y. Zhang, and T.J.R. Hughes. Isogeometric Fluid structure Inter-action Analysis with Applications to Arterial Blood Flow. Computational Mechanics, 38: 310–322, 2006. ISSN 0178-7675.

[4.] Y. Bazilevs, VM Calo, T.J.R. Hughes, and Y. Zhang. Isogeometric fluid-structure interaction: theory, algorithms, and computations. Computational mechanics, 43(1):3–37, 2008. ISSN 0178-7675.

[5.] H. G´omez, V.M. Calo, Y. Bazilevs, and T.J.R. Hughes. Isogeometric analysis of the Cahn-Hilliard phase-field model. Computer Methods in Applied Mechanics and Engineering, 197 (49-50):4333–4352, 2008. ISSN 0045-7825.

[6.] Y. Bazilevs, M.C. Hsu, I. Akkerman, S. Wright, K. Takizawa, B. Henicke, T. Spielman, and TE Tezduyar. 3d simulation of wind turbine rotors at full scale. part i: Geometry modeling and aerodynamics. International Journal for Numerical Methods in Fluids, 65(1-3):207–235, 2011.

[7.] Y. Bazilevs, M.C. Hsu, J. Kiendl, R. W¨uchner, and K.U. Bletzinger. 3d simulation of wind turbine rotors at full scale. part ii: fluid–structure interaction modeling with composite blades. International Journal for Numerical Methods in Fluids, 65(1-3):236-253, 2011.

[8.] T.J.R. Hughes, J.A. Cottrell, and Y. Bazilevs. Isogeometric analysis: CAD, finite elements, NURBS, exact geometry and mesh refinement. Computer Methods in Applied Mechanics and Engineering, 194:4135–4195, 2005.

[9.] J.A. Cottrell, A. Reali, Y. Bazilevs, and T.J.R. Hughes. Isogeometric analysis of structural vibrations. Computer Methods in Applied Mechanics and Engineering, 195(41-43):5257–5296, 2006.

[10.] T.J.R. Hughes, A. Reali, and G. Sangalli. Duality and unified analysis of discrete approximations in structural dynamics and wave propagation: comparison of p-method finite elements with k-method

NURBS. Computer methods in applied mechanics and engineering, 197(49-50):4104–4124, 2008. ISSN 0045-7825.
[11.] C.V. Verhoosel, M.A. Scott, T.J.R. Hughes, and R. de Borst. An Isogeometric Analysis Approach to Gradient Damage Models. Technical Report ICES REPORT 10-21, The Institute for Computational Engineering and Sciences, Austin, Texas, 2010.
[12.] A. Buffa, G. Sangalli, and R. V´azquez. Isogeometric analysis in electromagnetics: B-splines approximation. Computer Methods in Applied Mechanics and Engineering, 199(17-20):1143–1152, 2010. ISSN 0045-7825.
[13.] Y. Bazilevs, V.M. Calo, J.A. Cottrell, T.J.R. Hughes, A. Reali, and G. Scovazzi. Variational multiscale residual-based turbulence modeling for large eddysimulation of incompressible flows. Computer Methods in Applied Mechanics and Engineering, 197(1-4):173–201, 2007. ISSN 0045-7825.
[14.] Y. Bazilevs, C. Michler, V.M. Calo, and T.J.R. Hughes. Turbulence without Tears: Residual Based VMS, Weak Boundary Conditions, and Isogeometric Analysis of Wall-Bounded Flows. 2008.

ANNALS of Faculty Engineering Hunedoara – International Journal of Engineering